0026-895X/94/050866-07$03.00/0

MOLECULAR PHARMACOLOGY, 46:866-872, 1994.

Interaction of an Estramustine Photoaffinity Analogue with Cytoskeletal Proteins in Prostate Carcinoma Cells

LISA A. SPEICHER,[1] NAOMI LAING, LINDA R. BARONE, JOAN D. ROBBINS, KENNETH B. SEAMON, and KENNETH D. TEW

Department of Pharmacology, Fox Chase Cancer Center, Philadelphia, Pennsylvania 19111 (L.A.S., N.L., L.R.B., K.D.T.), and Center for Biologics Evaluation and Research, Food and Drug Administration, Bethesda, Maryland 20892 (J.D.R., K.B.S.)

Received November 5, 1993; Accepted July 27, 1994

SUMMARY

To identify specific drug targets of the antimitotic drug estramustine, a photoaffinity analogue, 17-*O*-[[2-[3-(4-azido-3-[^{125}I]iodophenyl)propionamido]ethyl]carbamyl]estradiol-3-*N*-bis(2-chloroethyl)carbamate, was synthesized and reacted in competition assays with cytoskeletal protein preparations. By attaching the photoaffinity ligand to the 17β-position of the steroid D-ring, the cytotoxic properties of the drug were maintained. In cytoskeletal protein preparations from human prostate carcinoma cells (DU 145) or a clonally selected, estramustine-resistant cell line (E4), the major microtubule-associated protein (MAP) present was MAP4. In both cytoskeletal fractions and reconstituted microtubules, 17-*O*-[[2-[3-(4-azido-3-[^{125}I]iodophenyl)propionamido]ethyl]carbamyl]estradiol-3-*N*-bis(2-chloroethyl)carbamate bound to both MAP4 and tubulin. From competition assays, the apparent binding constant for MAP4 from DU 145 cells was 15 μM. Similar calculations for tubulin gave values of 13 μM (bovine brain), 19 μM (DU 145 wild-type cells), and 25 μM (E4 cells). The identification of these cytoskeletal proteins as specific drug targets provides a direct explanation for the antimicrotubule and antimitotic effects of estramustine.

Estramustine, a chemotherapeutic agent used in combination treatment of advanced, hormone-refractory, prostate carcinoma (1, 2), demonstrates unusual pharmacological properties, with a mechanism of action distinct from the predicted alkylating or estrogen activities of its constituent moieties (3). The stability of the carbamate-ester bond linking nornitrogen mustard to estradiol is responsible for the unusual properties of the drug as well as its long clinical half-life (4). Estramustine should be classified as a microtubule poison, because it elicits cytotoxicity through microtubule disassembly and antimitotic activity (5–7).

Structural MAPs comprise a family of molecules defined by their ability to bind to tubulin and promote microtubule assembly *in vitro* (for review, see Refs. 8 and 9). The identification of different classes of MAPs, in addition to their tissue-, organ-, and species-specific distribution, suggests that specific MAPs may provide for specialized cellular functions of various microtubule subclasses. Although several classes, including MAP1, MAP2, τ (tau), and MAP4, have been characterized, the *in vivo* functions of these proteins are not completely understood.

Although previous studies utilizing radiolabeled estramustine and estramustine phosphate have documented the affinity of the drug for MAP1, MAP2, and τ (10), a direct analysis of estramustine binding to the variety of microtubule proteins has not been reported. The utility of photoaffinity analogue techniques in discriminating precise protein targets for a variety of agents is well documented. For example, direct photolabeling of tubulin with [^{3}H]GTP or [^{3}H]GDP (11), [^{3}H]colchicine or [^{3}H]podophyllotoxin (12), or [^{3}H]taxol (13) all demonstrated low but practical levels of label incorporation into β- or α-tubulin subunits. In many cases, increased efficiency of label incorporation is achieved by the attachment of a photoactivatable aromatic azide group to the drug. Such an approach has been useful in determining P-glycoprotein-specific binding of drugs such as vinblastine (14), verapamil (15), and forskolin (16). The latter study utilized the same photoaffinity ligand precursor used in this study, except that for estramustine the 17β-hydroxyl moiety proved an amenable substitution site. The same site has been used previously for the attachment of dansyl chloride, to permit visualization of drug uptake and cellular distribution (17). In that study the drug, although more hydrophobic, maintained its cytotoxic and antimicrotubule properties. A similar result is now reported for the photoaffinity analogue of estramustine.

This work was supported by National Institutes of Health Grant R35-CA53893 and a grant from the Helsingborg Research Foundation.

[1] Present address: U.S. Bioscience, Inc., 1 Tower Bridge, 100 Front Street, 4th Floor, West Conshohocken, PA 19428.

ABBREVIATIONS: MAP, microtubule-associated protein; AIPP-EM, 17-*O*-[[2-[3-(4-azido-3-iodophenyl)propionamido]ethyl]carbamyl]estradiol-3-*N*-bis(2-chloroethyl)carbamate; 17-AEC-EM, 17β-(2-aminoethylaminocarbonyl)estramustine; AIPPS, *N*-succinimidyl(4-azido-3-iodophenyl)propionate; PBS, phosphate-buffered saline; DTT, dithiothreitol; PMSF, phenylmethylsulfonyl fluoride; TLC, thin layer chromatography; SDS, sodium dodecyl sulfate; PAGE, polyacrylamide gel electrophoresis; TBS-T, Tris-buffered saline with Tween; PIPES, piperazine-*N*,*N*′-bis(2-ethanesulfonic acid); EGTA, ethylene glycol bis(β-aminoethyl ether)-*N*,*N*,*N*′,*N*′-tetraacetic acid.

The ability of tumors to develop resistance to drugs used for treatment remains a major obstacle to successful cancer chemotherapy. Selection of estramustine-resistant cells was a prerequisite to determining the selective adaptive traits that constitute the drug-resistant phenotype, in addition to gaining insight into the mechanism(s) of action of this drug. Our previous data (18, 19) suggested a resistance profile dissimilar from those typically seen for microtubule poisons. The present study was designed to identify those microtubule proteins that are specific targets for estramustine. The importance of this approach is enhanced by the recent report (20) that suggests that MAP binding may not be critical to the cytotoxic mechanism of estramustine. The results suggest that both tubulin and MAP4 are targets for estramustine, with apparent binding constants consistent with those drug concentrations that are required to cause antimitotic effects.

Experimental Procedures

Cell culture. The human prostatic carcinoma cell line (DU 145) was cultured and the estramustine-resistant subclone (E4) was selected as described previously (19). The selection of estramustine-resistant lines resulted in a clone exhibiting approximately 5-fold increased estramustine resistance, compared with wild-type drug-sensitive cells.

Cytotoxicity measurements. Estramustine-sensitive and -resistant cells were plated at a density of 300 cells/9.6-cm^2 well in six-well plates containing the appropriate drug concentration. Each six-well plate represented one drug concentration. The plates were incubated undisturbed at 37° in a humidified 5% CO_2 atmosphere for a minimum of 10 days. The cells were then rinsed with PBS, fixed in 95% ethanol for 30 min, rinsed with PBS, stained with 0.1% crystal violet for 45 min, and rinsed with water to remove excess stain. The colonies (>28 cells) were counted manually, and the percentage of cell survival was determined by comparing the number of drug-treated cells with the number of cells in the control wells. Plating efficiency was determined to be between 35 and 40%.

Microtubule protein purification. Microtubule protein was isolated from cells following a modification of the taxol-dependent procedure of Vallee (21). Briefly, cells grown to 80% confluency in 150-mm^2 dishes were washed once in PBS, dissociated from the dishes, and harvested by centrifugation at 2500 rpm for 10 min. The cell pellet was washed twice in PBS by centrifugation and was resuspended in an equal volume of microtubule-stabilizing buffer (0.1 M PIPES, 5.0 mM $MgCl_2$, 5.0 mM EGTA, 1.0 mM DTT) containing protease inhibitors (100 μg/ml aprotonin, 1 mM PMSF, 1% leupeptin, 100 μg/ml soybean trypsin inhibitor). The cells were homogenized with 20 strokes in a 5-ml Teflon/glass homogenizer (Wheaton Instruments Division, Millville, NJ) on ice and centrifuged at 100,000 × *g* for 30 min at 4°. The supernatant was removed and transferred to a glass tube. Microtubules were reassembled by addition of 5 mM (5′-adenylylinidodiphosphate), 1 mM GTP, and 10 μM taxol to the supernatant and incubation of the mixture at 37° for 45 min. The mixture was then layered over a sucrose cushion and centrifuged at 100,000 × *g* for 30 min at 37°. The final microtubule pellet was resuspended in microtubule-stabilizing buffer with protease inhibitors, divided into aliquots, and stored at −80° until use.

Synthesis of 17β-amino intermediate. 17-AEC-EM was synthesized by a procedure similar to that described by Robbins *et al.* (22). To 100 mg (0.228 mmol) of estramustine dissolved in 500 μl of methylene chloride, 74 mg (0.456 mmol) of 1,1′-carbonyldiimidazole were added and the reaction was stirred at room temperature for 1.5 hr. Ethylenediamine (0.456 mmol) was added and the reaction was stirred for another 2 hr at room temperature. The reaction mixture was diluted in methylene chloride, washed once with water, and then dried *in vacuo*. The product was purified on a 6-g silica gel (10 μm; Analtech) column in chloroform/methanol/ammonia (9:1:1). The product was detected on silica gel TLC plates developed in the same solvent system but was detected by UV fluorescence and by trinitrobenzene sulfonic acid spray, which shows the existence of free amines [^{1}H NMR ($CDCl_3$): δ 7.29 (d, 1 H, phenyl), 6.88 (dd, 1 H, phenyl), 6.83 (s, 1 H, phenyl), 5.36 (s, 1 H, OH), 4.62 (t, 1 H, H17), 3.83 (t, 2 H, CH_2CH_2Cl), 3.76 (t, 2 H, CH_2CH_2Cl), 3.74 (s, 4 H, CH_2Cl), 3.31 (m, 4 H, H16 and CH_2CH_2NHCO), 2.93 (t, 2 H, $CH_2CH_2NH_2$), 2.86 (d, 1 H, H16), and 0.81 (s, 3 H, CH_3)].

Synthesis of the photoaffinity label [^{125}I]AIPP-EM. [^{125}I]AIPPS (250 μCi) was concentrated to dryness under N_2. Twenty-five microliters of a solution of 17-AEC-EM (5 mg/ml) in methylene chloride were added to the reaction vial and allowed to react overnight at room temperature. The reaction was monitored by TLC (with ethyl acetate as the developing solvent) and was visualized by autoradiography. The reaction mixture was applied to a 1-g silica gel column equilibrated with ethyl acetate. Fractions were collected and monitored by TLC, followed by autoradiography. The fractions corresponding to iodinated estramustine were pooled, concentrated, and stored at −20° in ethanol. Labeled estramustine was separated from free estramustine under these conditions, and therefore the specific activity of the labeled compound (Fig. 1) was considered to be equal to that of the [^{125}I]AIPPS reagent (2175 Ci/mmol).

Synthesis of 4-[3-(4-hydroxyphenyl)propionamido]-*N*-17β-(2-aminoethylaminocarbonyl)estramustine. A 2-fold excess of *N*-succinimidyl-3-(4-hydroxyphenyl)propionate was added to 17-AEC-EM dissolved in a small volume of dimethylformamide. The reaction was stirred at room temperature for 16 hr. The crude product was dried under vacuum and applied to a 6-g column of silica gel in ethyl acetate. The fractions were monitored by UV fluorescence, pooled, and dried [^{1}H NMR: δ 7.31 (d, 1 H, phenyl, estramustine), 7.10 [d, 1 H, phenyl, (4-hydroxyphenyl)propionamide], 6.95 (dd, 1 H, phenyl, estramustine), 6.90 (s, 1 H, phenyl, estramustine), 6.09 [s, 1 H, phenyl, (4-hydroxyphenyl)propionate], 6.09 [s, 1 H, OH, (4-hydroxyphenyl)propionamide], 5.09 (s, 1 H, OH, estramustine), 4.69 (t, 2 H, H17), 3.92 (t, 2 H, CH_2CH_2Cl), 3.87 (t, 2 H, CH_2CH_2Cl), 3.82 (s, 2 H, CH_2Cl), 3.39 ($HNCH_2CH_2NHCO$), 3.31 (d, 2 H, H16), 3.30 [t, 2 H, CH_2CH_2NHCO, (4-hydroxyphenyl)propionamide], 2.95 (m, H16 and CH_2CH_2NHCO), and 0.87 (s, 3 H, CH_3)].

Photoaffinity labeling. Microtubule proteins were preincubated on ice for 30 min in buffer alone (10 mM Tris·HCl, pH 7.4) or buffer containing competing drug (100 μM estramustine or 100 μM estramustine phosphate). ^{125}I-Estramustine was added to the microtubule proteins (1 × 10^6 cpm/assay), and the samples were incubated on ice in the dark for 30 min. The samples were then photolyzed (200,000 μJ) in a Stratagene UV Stratalinker, and 1% β-mercaptoethanol was added as a scavenger of long-lived species. Labeled proteins were then prepared for gel electrophoresis. Gels were dried and exposed to XAR-5 film at −80° for 3 days or less. The films were then scanned and spots were quantitated using an Ultrascan XL laser densitometer (Pharmacia LKB Biotechnology, Piscataway, NJ). To determine the ability of unlabeled estramustine to inhibit the photolabeling of tubulin from different sources, log dose-response curves were plotted to obtain "apparent" IC_{50} values for estramustine competition. Values obtained represent the mean ± standard deviation of at least three experiments.

Bovine brain tubulin purification. Microtubule proteins were prepared from bovine brains by a pH- and temperature-dependent method (23). The twice-cycled microtubule pellet obtained was resus-

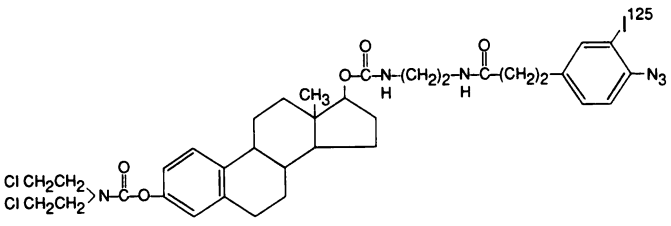

Fig. 1. Structure of the photoaffinity analogue [^{125}I]AIPP-EM.

pended in an equal volume of PEM (0.1 M Na-PIPES, pH 6.6, 1 mM EGTA, 1 mM $MgSO_4$, 0.1 mM GTP) and stored on ice for 2 hr. Tubulin was separated from the MAPs by DEAE-Sephadex column chromatography (24). Column fractions were analyzed by SDS-PAGE and Western blot analysis with an anti-β-tubulin monoclonal antibody. Appropriate fractions were combined and dialyzed for 16 hr against PEM, pH 7.4, containing 0.1 mM PMSF, 1 μg/ml leupeptin, 1 μg/ml pepstatin, and 1 μg/ml trypsin inhibitor.

Western blot analysis. Gels were transferred to nitrocellulose membranes by electroblotting. Membranes were incubated for 1 hr in TBS-T (with 3% milk) to reduce nonspecific binding of antisera. Blots were washed three times (10 min each) with TBS-T (50 mM tris. HCl, pH 7.5, 400 mM NaCl and 0.05% tween-20), followed by incubation with primary antibody in 0.5% bovine serum albumin/TBS-T for 2 hr at 25°. Blots were rinsed three times (10 min each) with TBS-T and incubated for 1.5 hr at 25° with a horseradish peroxidase-conjugated secondary antibody. Blots were rinsed three times (10 min each) with TBS-T and developed with the horseradish peroxidase developer diaminobenzidine.

MAP4/tubulin purification. A MAP4-enriched fraction was isolated from wild-type DU 145 cells by a heat treatment method (25). Briefly, cell pellets were resuspended in an equal volume of cold PEM, pH 6.9, containing 1 mM GTP, 1 mM DTT, and 1 mM PMSF and were homogenized on ice using 40 strokes. After centrifugation at 30,000 × *g* for 20 min at 4°, the supernatant was removed and centrifuged at 100,000 × *g* for 1 hr at 4°. The supernatant was then boiled for 5 min, chilled on ice for 15 min, and centrifuged at 30,000 × *g* for 40 min at 4°, to remove denatured protein. The resulting supernatant was a thermostable extract enriched in MAP4 and was concentrated by vacuum dialysis against PEM, pH 6.9, containing 0.1 mM PMSF, 1 μg/ml leupeptin, and 1 μg/ml pepstatin. The thermostable extract was then mixed with DEAE-purified bovine brain tubulin, and 8% dimethylsulfoxide and 1 mM GTP were added to promote polymerization. After incubation at 37° for 30 min, the mixture was centrifuged at 30,000 × *g* for 30 min at 37°. The hybrid microtubule pellet was stored on ice for 1 hr, resuspended in PEM, pH 7.4, and then used for photoaffinity analogue studies.

Tubulin was purified from wild-type and resistant (E4) DU 145 cells by a modified pH- and temperature-dependent cycling method (23), followed by DEAE-Sephadex column chromatography. Briefly, cell pellets were resuspended in an equal volume of cold 100 mM PIPES, pH 7.4, 4 mM EGTA, 1 mM $MgSO_4$, 0.5 mM DTT, 0.1 mM PMSF, and were homogenized on ice with 40 strokes. The homogenate was centrifuged at 39,000 × *g* for 1 hr at 4° and the pellet was discarded. To promote microtubule assembly, 8% dimethylsulfoxide and 1 mM GTP (final concentrations) were added to the supernatant, which was incubated at 37° for 45 min. Microtubules were pelleted by centrifugation at 39,000 × *g* for 30 min at 37° and the supernatant was discarded. The pellets were incubated on ice for 15 min before resuspension in cold PEM, pH 6.9, with 1 mM PMSF. The protein suspension was sonicated (2 × 30 sec) on ice and incubated on ice for another 15 min to maximize depolymerization. The depolymerized microtubules were clarified by centrifugation at 39,000 × *g* for 30 min at 4°. NaCl (final concentration, 0.25 M) was added to the clarified supernatant in preparation for column chromatography. DEAE-Sephadex chromatography was performed according to the method of Vallee (24), to separate tubulin from the MAPs. Column fractions were analyzed by SDS-PAGE, followed by silver staining and Western blot analysis. Tubulin-containing fractions were combined, dialyzed against 10 mM Tris·HCl, pH 7.4, containing 0.1 mM PMSF, 1 μg/ml leupeptin, 1 μg/ml pepstatin, and 1 μg/ml trypsin inhibitor, and then used for photoaffinity analogue studies.

Results

The cytotoxicity of the unlabeled synthetic intermediate AIPP-EM and estramustine is shown in Fig. 2. Both compounds caused cell death in wild-type DU 145 and estramustine-resistant E4 cells. Approximately 2-fold resistance to the precursor was expressed by the E4 cells, a value slightly less than the 4–5-fold resistance to estramustine. On a molar basis, the IC_{50} values of both the precursor and AIPP-EM were approximately equivalent to that of estramustine in the wild-type cells. For E4 cells, the precursor was more cytotoxic, perhaps reflecting its enhanced hydrophobic nature. However, overall these data suggested that AIPP-EM maintains the essential cytotoxic characteristics of the parent drug.

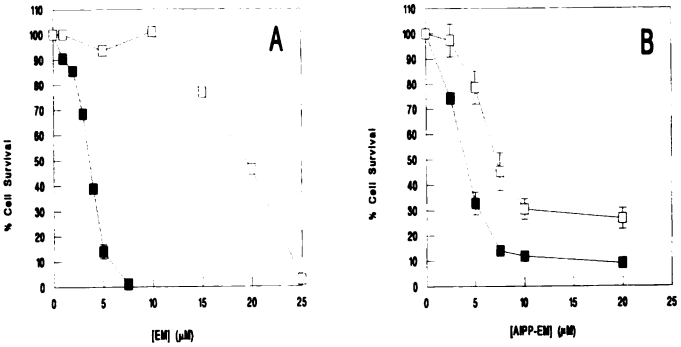

Fig. 2. Cytotoxicity of estramustine and estramustine photoaffinity analogue in DU 145 wild-type or E4 cells. Survival was estimated as described in Experimental Procedures. Estramustine (*EM*) (A) and nonradioactive AIPP-EM (B) were tested with DU 145 (■) and E4 (□) cells.

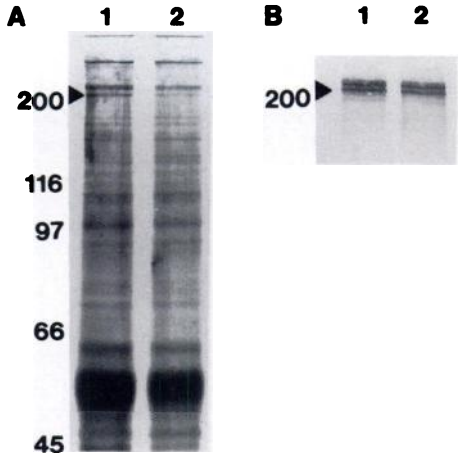

Fig. 3. A, Silver-stained SDS-PAGE of microtubule protein extracts (20 μg) isolated from wild-type (*lane 1*) and resistant (E4) (*lane 2*) DU 145 cell lines. B, Western blot, *Arrowhead*, approximately 200-kDa protein that immunoreacts with the anti-MAP4 polyclonal antibody. *Lane 1*, wild-type cells; *lane 2*, E4 cells. *Numbers*, molecular masses (in kDa).

Microtubule proteins from the wild-type and E4 cells were prepared and separated by 8% SDS-PAGE. Fig. 3A shows a silver stain of the gel. As expected, tubulin was the most prominent protein (band at ~50 kDa) obtained from the preparation. The doublet at an apparent molecular mass of 200 kDa was identified, through Western blot analysis, as MAP4 (Fig. 3B). Although silver stain does not permit linear quantification, the immunoblot did not suggest any significant difference in MAP4 expression between the wild-type and resistant cells.

The photoaffinity analogue of estramustine was used to identify potential microtubule protein targets in these same cell extracts. After an initial preincubation with either drug-free buffer, 100 μM estramustine, or 100 μM estramustine phosphate, isolated microtubule proteins were incubated with [^{125}I]AIPP-EM and then separated on denaturing 8% polyacryl-

amide gels. Labeled proteins, detected by autoradiography, are shown in Fig. 4. Although a number of proteins were labeled by [^{125}I]AIPP-EM, competitive inhibition of labeled drug binding in the presence of excess unlabeled estramustine was seen only for a protein with a molecular mass of 210 kDa. The photoaffinity analogue was consistently competed from this protein by estramustine in both cell lines and also in two other resistant clones (data not shown). The more polar estramustine phosphate had no inhibitory effect on label binding. Confirmation of the specificity of [^{125}I]AIPP-EM binding to the 210-kDa protein was provided by the consistency of labeling in 15 separate experiments and competition by unlabeled estramustine. Although a number of other proteins were also labeled, neither estramustine nor estramustine phosphate interfered with this labeling at the protein concentrations used in this experiment.

Most strongly labeled of the separated proteins was a band at approximately 55 kDa. This band was recognized by a monoclonal antibody to β-tubulin, and in these prostate cells tubulin is the most abundant of the microtubule proteins expressed. Thus, it was not surprising that the highest level of [^{125}I]AIPP-EM binding was to tubulin.

For confirmation that these protein bands were tubulin and MAP4, purified bovine tubulin was used to "purify" MAP4 from DU 145 cells. The hybrid microtubule preparations are shown in Fig. 5. The Western blot (Fig. 5B) illustrates the reactivity of the purified bovine tubulin preparation with a monoclonal antibody to β-tubulin, yielding a predominant band at ~55 kDa and a minor band at ~110 kDa, representing the tubulin dimer (Fig. 5B, *lane 1*). Fig. 5B, *lane 2*, represents the MAP4-enriched extract from DU 145 cells, with reactivity at ~210 kDa with a polyclonal antibody to MAP4, whereas Fig. 5B, *lane 3*, represents the hybrid microtubules with the presence of both tubulin and MAP4. When [^{125}I]AIPP-EM was reacted with these purified proteins, all three were labeled by the drug. By titration with increasing concentrations of unlabeled estramustine, competitive inhibition of binding was found for all three of the bands. A few anomalies were apparent. For example, although 20–50 μM estramustine essentially eliminated [^{125}I]AIPP-EM binding to MAP4 and significantly reduced binding to tubulin, there was a measurable increase in binding to both monomeric and dimeric tubulin at the higher concentrations (75 and 100 μM). There was also evidence of drug binding to a protein at 35 kDa, especially when competitive estramustine concentrations of >20 μM were used. The apparent increase in photolabeling of the 35-kDa band and of tubulin observed at higher unlabeled estramustine concentrations may reflect increased labeling of nonspecific or low affinity sites because the photolabel is displaced from the high affinity

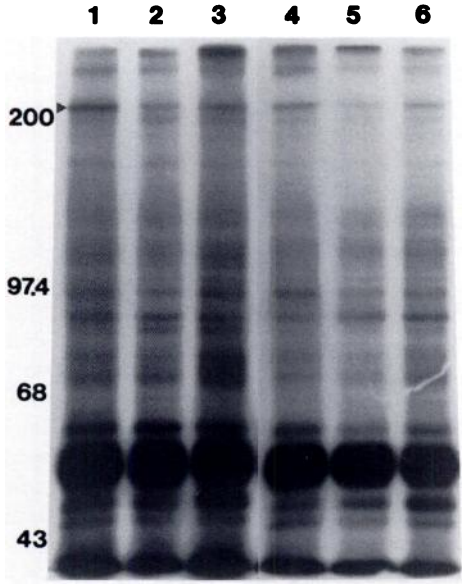

Fig. 4. Photolabeling by [^{125}I]AIPP-EM of microtubule proteins isolated from wild-type and E4 cells. Microtubule protein (50 μg) from wild-type (*lanes 1-3*) or E4 (*lanes 4-6*) cells was preincubated with buffer alone (*lanes 1* and *4*), 100 μM estramustine (*lanes 2* and *5*), or 100 μM estramustine phosphate (*lanes 3* and *6*). Proteins were incubated with [^{125}I]AIPP-EM, photolyzed, separated on 8% polyacrylamide gels, and analyzed by autoradiography as described in Experimental Procedures. Photolabeling of a protein of ~200 kDa (*arrowhead*) was consistently inhibited by excess unlabeled estramustine in extracts from both cell lines. No such competition was observed with estramustine phosphate.

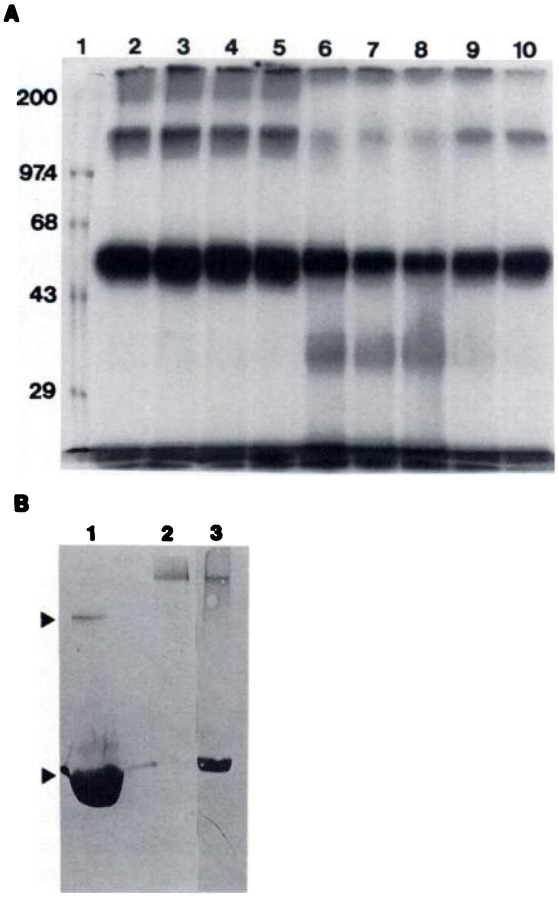

Fig. 5. A, Photolabeling of reconstituted microtubules separated by 8% SDS-PAGE. Bovine tubulin was used to purify MAP4 from wild-type DU 145 cells (see Experimental Procedures). Large molar excesses of bovine tubulin were used to facilitate purification of MAP4. Competitive concentrations of unlabeled estramustine were as follows: *lane 1*, molecular mass markers; *lane 2*, 0 μM; *lane 3*, 0.1 μM; *lane 4*, 1.0 μM; *lane 5*, 10 μM; *lane 6*, 20 μM; *lane 7*, 30 μM; *lane 8*, 50 μM; *lane 9*, 75 μM; *lane 10*, 100 μM. B, *Lane 1*, Western blot of purified bovine brain tubulin probed with a monoclonal antibody to β-tubulin. Monomeric and dimeric bovine tubulin bands are apparent (*arrowheads*). *Lane 2*, Western blot of the MAP4-enriched extract from DU 145 cells probed with anti-MAP4 polyclonal antibody. *Lane 3*, Western blot of the microtubule pellet from the polymerization of bovine tubulin with the MAP4 extract, probed with both anti-β-tubulin and anti-MAP4 antibodies. A and B represent different gels run for different lengths of time, and therefore the tubulin bands exhibited different migration rates.

estramustine binding site and is free to label nonspecific sites on any of the proteins present in the hybrid microtubules. Tubulin constituted >90% of the total protein in these gels and was present at a concentration of ~1 μM. Such an excess of tubulin was needed to bind and purify sufficient MAP4 from the DU 145 cells. However, for subsequent gels comparing drug binding to bovine and human tubulin, 0.03–0.1 μM concentrations of purified tubulin were used and there was no evidence of the additional bands shown in Fig. 5. In addition, nonspecific or low affinity labeling of tubulin was not observed at higher concentrations of competing estramustine, presumably because of the low tubulin concentrations used. For example, Fig. 6 compares estramustine competition with [^{125}I]AIPP-EM binding to purified tubulin from bovine brain (Fig. 6A), DU 145 wild-type cells (Fig. 6B), and E4 cells (Fig. 6C). Through densitometric scanning, the ability of estramustine to compete with the labeling by [^{125}I]AIPP-EM was quantitated to yield apparent IC_{50} values, which were as follows: bovine tubulin, 15.9 ± 6.3 μM; DU 145 cell tubulin, 19.5 ± 2.3 μM; E4 cell tubulin, 24.6 ± 2.3 μM (mean ± standard deviation). In some experiments, drug binding to tubulin dimers was apparent. When this was found, the diminution of label with increasing concentrations of unlabeled estramustine mirrored that for the monomer. The extent of labeling of the dimer was always significantly less than that of the monomer, reflecting the smaller amounts of dimer formed.

Fig. 7 illustrates the effect of the photolysis procedure on covalent dimerization of tubulin. Even in the absence of the photoaffinity analogue, Fig. 7, *lane 2*, shows that photolysis led to low levels of dimerization, as indicated by the appearance of an anti-β-tubulin antibody-positive band at ~110 kDa (Fig. 7, *upper arrowhead*). Fig. 7, *lane 6*, shows that [^{125}I]AIPP-EM bound to this dimer. In fact, there was some indication that even the presence of such low concentrations of the photoaffinity analogue may have enhanced the extent of covalent dimerization as a consequence of photolysis (Fig. 7, *lane 4*).

Discussion

Photoaffinity ligands have proved useful in delineating polypeptide target specificity of a number of tubulin-binding agents. Antimitotic and antimicrotubule effects consistent with these tubulin-binding agents have been shown to be similar to, but distinct from, the cytotoxic consequences of estramustine (7). Both the parent drug and the water-soluble, clinically administered, form of estramustine have been shown through a variety of methods to bind to MAP1, MAP2, and τ with binding constants in the range of 10–20 μM, contingent upon the assay conditions and the nature of the isolated MAP used (5, 10, 26).

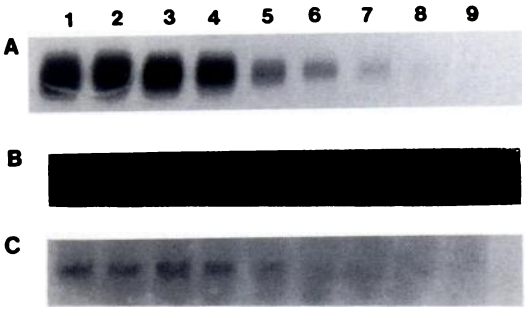

Fig. 6. Photolabeling of tubulin purified from bovine brain (A), DU 145 wild-type cells (B), and E4 cells (C). Increasing concentrations of unlabeled estramustine were used with 1 nM [^{125}I]AIPP-EM and 0.03–0.1 μM tubulin. A, Drug concentrations were as follows: *lane 1*, 0 μM; *lane 2*, 0.1 μM; *lane 3*, 1 μM; *lane 4*, 10 μM; *lane 5*, 20 μM; *lane 6*, 30 μM; *lane 7*, 50 μM; *lane 8*, 75 μM; *lane 9*, 100 μM. B and C, Drug concentrations were as follows: *lane 1*, 0 μM; *lane 2*, 0.1 μM; *lane 3*, 1 μM; *lane 4*, 10 μM; *lane 5*, 25 μM; *lane 6*, 35 μM; *lane 7*, 50 μM; *lane 8*, 75 μM; *lane 9*, 100 μM. Data are representative blots from at least three experiments.

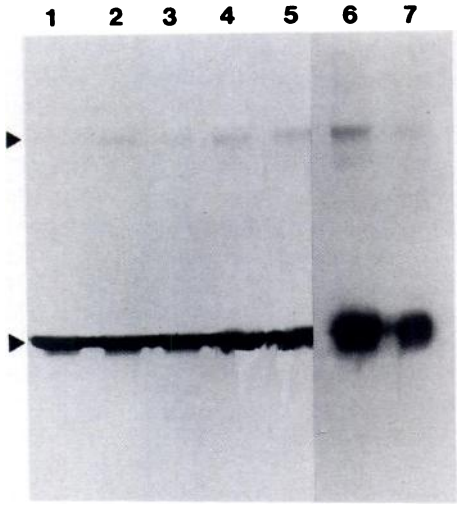

Fig. 7. Effect of photolysis on tubulin polymerization. Purified bovine tubulin (see Experimental Procedures) was subjected to SDS-PAGE separation in the presence or absence of drug, before and after exposure to 200,000-μJ light energy. *Lanes 1-5*, Western blot with anti-β-tubulin monoclonal antibody; *lanes 6* and *7*, autoradiogram showing [^{125}I]AIPP-EM binding. *Arrowheads*, tubulin monomer and dimer. *Lane 1*, no photolysis; *lanes 2-5*, with photolysis; *lane 2*, no estramustine; *lane 3*, with 50 μM estramustine; *lane 4*, with 1 nM [^{125}I]AIPP-EM; *lane 5*, with 50 μM estramustine and 1 nm [^{125}I]-AIPP-EM; *lanes 6* and *7*, equivalent autoradiogram from *lanes 4* and *5*.

Notwithstanding these earlier *in vitro* reports, the present photoaffinity analogue data provide evidence that MAP4 is both a primary tumor MAP in the DU 145 prostate carcinoma cell line and a drug target, as judged by the estramustine competitive binding assays. It is noteworthy that the presence of a phosphate moiety in the 17β-position of estramustine eliminated the ability of the drug to compete with the photoaffinity labeling, presumably as a consequence of the increased negative charge and enhanced hydrophilic properties of estramustine phosphate. Other studies (10) have suggested that *in vitro* data obtained with estramustine phosphate cannot be duplicated when estramustine is used. Such a concept is supported by our present observations and suggests that the differences in charge and solubility may have a substantial impact upon the binding specificities of the drugs. Although a number of detailed *in vitro* studies have utilized estramustine phosphate, it is apparent that rapid dephosphorylation occurs *in vivo* and, indeed, is a prerequisite for cellular uptake, because the polar nature of the phosphate group prevents membrane traversal. Thus, the pharmacological properties and target specificity of the hydrophobic photoaffinity ligand may more closely match those of the active parent drug, estramustine. This would be consistent with the observation that the photoaffinity analogue maintains cytotoxicity. In fact, our previous studies showed that attachment of a fluorescent dansyl chloride substituent at the 17β-position of estramustine produced only a slight quantitative alteration of its antimicrotubule properties (17).

Direct binding of estramustine to tubulin has been suggested

to play a role in the antimitotic properties of the drug (20). It is apparent that estramustine binding to the cellular tubulin component is comparatively high; this is not surprising, because tubulin is the most prevalent of the microtubule proteins. We have found it possible to demonstrate direct photolabeling of tubulin using [^{3}H]estramustine (data not shown). However, the efficiency of this approach is limited by the specific activity of the tritiated drug and the lower sensitivity of tritium detection. Thus, the synthesis and testing of the photoaffinity analogue permitted enhanced sensitivity in detecting protein binding.

A few experimental anomalies or artifacts were apparent in some of the photoaffinity gels. These occurred when high levels of hybrid microtubules were used with high concentrations of unlabeled estramustine. In Fig. 5, 75 and 100 μM concentrations of competitive estramustine appeared to cause an increase in [^{125}I]AIPP-EM binding to both the tubulin monomer and dimer bands. This effect was not seen in subsequent experiments when lower tubulin concentrations (0.03–0.1 μM) were used (Fig. 6). A possible explanation could be that increased nonspecific labeling was observed when [^{125}I]AIPP-EM was displaced from its high affinity site(s) on tubulin by high concentrations of estramustine and was then free to interact with any nonspecific sites present on tubulin. This effect was observed only when the tubulin concentrations were high enough to allow a significant low affinity interaction between "displaced" [^{125}I]AIPP-EM and tubulin. A second anomaly was the appearance of [^{125}I]AIPP-EM binding to a lower molecular mass band (~35 kDa) at 20–50 μM concentrations of competitive estramustine, which reduced labeling of both tubulin monomer and dimer. It is possible that this 35-kDa protein was labeled when a significant portion of the label was displaced from its high affinity binding site on tubulin by estramustine but was not labeled at the highest concentrations of estramustine (75 and 100 μM) because [^{125}I]AIPP-EM was completely inhibited from labeling this protein by estramustine. This 35-kDa protein most likely represents a microtubule protein with an "intermediate" affinity for estramustine.

The binding constants of other antimicrotubule drugs for tubulin are generally 1–3 log units lower than those we report for estramustine. Indeed, although many of the antimicrotubule effects that are produced by estramustine are consistent with those of standard tubulin-binding agents, the cytotoxicity profiles are distinct (7). In addition, the synergistic antimitotic and cytotoxic effects of estramustine in combination with vinblastine (26) or taxol (19) argue against duplicate or overlapping effects, because purely additive antimicrotubule and cytotoxic effects would then be predicted. Thus, the antimicrotubule and antimitotic properties of estramustine could conceivably be the product of the combined MAP and tubulin binding.

The resistant cell lines, cultured in the continued presence of estramustine, have acquired a number of morphological adaptations. The cells are smaller, have slightly slower doubling times, and traverse mitosis more quickly. Concomitantly, their mitotic spindles are smaller and they are approximately half-aneuploid, compared with the wild-type cell line (18, 27). Although the present data reveal a difference in the apparent binding constants of estramustine for tubulin (as determined from the ability of estramustine to prevent labeling by [^{125}I] AIPP-EM) from the wild-type (19.5 μM) and E4 (24.6 μM) cells, it is not presently clear whether this is a major factor contributing to the resistant phenotype. There are subsequent changes in the total transcript levels of cytoskeletal elements in the resistant cells. Approximately 20-fold more mRNA for β-tubulin and MAP4 is found in E4 cells, compared with wild-type cells (data not shown). This may indicate that multiple differences in microtubule regulation and organization may contribute to the resistant phenotype.

Griseofulvin, a widely used antifungal agent, has also been suggested to bind to MAPs and tubulin (28–31). Resistance to this agent in Chinese hamster ovary cells has been found to be accompanied by the concomitant appearance of a putative 180-kDa MAP, resulting from a mutation in the structural gene coding for a 200-kDa MAP (30), and in a different cell line by changes in β-tubulin subunits (31). Considering the critical role of MAP4 in mitosis and the importance of post-translational modifications in enacting mitotic progression (32), the affinity of estramustine for this MAP may be detrimental to cell cycle progression and may contribute to the antimitotic properties of the drug. Alternatively, the direct interaction of the drug with tubulin may be sufficient to account for the antimitotic properties of the drug. Whichever of these mechanisms predominates, regulation of the synthesis of tubulin and/or MAP4 may be an adaptation that permits the resistant cells to circumvent the effects of the drug or may be a consequence of exposure to estramustine.

Acknowledgments

We are considerably indebted to Dr. Joanna Olmsted for the generous provision of antibodies to and a cDNA probe for MAP4 and to Dr. Tim Yen for the probes for α- and β-tubulin.

References

1. Hudes, G. R., R. Greenberg, R. L. Krigel, S. Fox, R. Scher, S. Litwin, P. Watts, L. Speicher, K. D. Tew, and R. Comis. Phase II study of estramustine and vinblastine, two microtubule inhibitors, in hormone refractory prostate cancer. *J. Clin. Oncol.* **10**:1754–1761 (1992).
2. Seidman, A., H. I. Scher, D. Petrylak, D. D. Dershaw, and T. Curley. Estramustine and vinblastine: use of prostate specific antigen as a clinical trial end point for hormone refractory prostate cancer. *J. Urol.* **147**:931–934 (1992).
3. Tew, K. D. The mechanism of action of estramustine. *Semin. Oncol.* **10**:21–26 (1983).
4. Gunnarsson, P. O., and G. P. Forshell. Clinical pharmacokinetics of estramustine phosphate. *Urology* **23**:22–27 (1984).
5. Stearns, M., M. Wang, K. D. Tew, and L. I. Binder. Estramustine binds a MAP-1-like protein to inhibit microtubule assembly *in vitro* and disrupt microtubule organization in DU 145 cells. *J. Cell Biol.* **107**:2647–2656 (1988).
6. Moraga, D., A. Rivas-Berrios, G. Farias, M. Wallin, and R. B. Maccioni. Estramustine-phosphate binds to a tubulin binding domain on microtubule-associated proteins MAP-2 and *tau*. *Biochim. Biophys. Acta* **1121**:97–103 (1992).
7. Tew, K. D., J. P. Glusker, B. Hartley-Asp, G. Hudes, and L. A. Speicher. Preclinical and clinical perspectives on the use of estramustine as an antimitotic drug. *Pharmacol. Ther.* **56**:323–339 (1992).
8. Olmsted, J. B. Microtubule-associated proteins. *Annu. Rev. Cell Biol.* **2**:421–457 (1986).
9. Olmsted, J. B. Non-motor microtubule-associated proteins. *Curr. Opin. Cell Biol.* **3**:52–58 (1991).
10. Friden, B., M. Rutberg, J. Deinum, and M. Wallin. The effect of estramustine derivatives on microtubule assembly *in vitro* depends on the charge of the substituent. *Biochem. Pharmacol.* **42**:997–1006 (1991).
11. Nath, J. P., G. R. Eagle, and R. H. Himes. Direct photoaffinity labeling of tubulin with guanosine 5′-triphosphate. Biochemistry **24**:1555–1560 (1985).
12. Wolff, J., L. Knipling, H. J. Cahnmann, and G. Palumbo. Direct photoaffinity labeling of tubulin with colchicine. *Proc. Natl. Acad. Sci. USA* **88**:2820–2824 (1991).
13. Rao, S., H. Band, and I. Ringel. Direct photoaffinity labelling of tubulin with taxol. *J. Natl. Cancer Inst.* **84**:785–788 (1992).
14. Safa, A. R., C. J. Glover, M. B. Meyers, J. L. Biedler, and R. L. Felsted. Vinblastine photoaffinity labeling of a high molecular weight surface membrane glycoprotein specific for multidrug-resistant cells. *J. Biol. Chem.* **261**:6137–6140 (1986).
15. Qian, X.-D., and W. T. Beck. Binding of an optically pure photoaffinity analogue of verapamil, LU-49888, to P-glycoprotein from multidrug-resistant human leukemic cell lines. *Cancer Res.* **50**:1132–1137 (1990).
16. Morris, D. I., J. D. Robbins, A. E. Ruoho, E. M. Sutkowski, and K. B.

Seamon. Forskolin photoaffinity labels with specificity for adenylyl cyclase and the glucose transporter. *J. Biol. Chem.* **266**:13377–13384 (1991).
17. Stearns, M. E., D. P. Jenkins, and K. D. Tew. Dansylated estramustine, a novel probe for studies of uptake and identification of intracellular targets. *Proc. Natl. Acad. Sci. USA* **82**:8483–8487 (1985).
18. Speicher, L. A., V. R. Sheridan, A. Godwin, and K. D. Tew. Resistance to the antimitotic drug estramustine is distinct from the multidrug resistant phenotype. *Br. J. Cancer* **64**:267–273 (1991).
19. Speicher, L. A., L. Barone, and K. D. Tew. Combined antimicrotubule activity of estramustine and taxol in human prostatic carcinoma cell lines. *Cancer Res.* **52**:4433–4440 (1992).
20. Dahllof, B., A. Billstrom, F. Cabral, and B. Hartley-Asp. Estramustine depolymerizes microtubules by binding to tubulin. *Cancer Res.* **53**:4573–4581 (1993).
21. Vallee, R. B. A taxol-dependent procedure for the isolation of microtubules and microtubule-associated proteins (MAPs). *J. Cell Biol.* **92**:435–442 (1982).
22. Robbins, J. D., A. Laurenza, R. W. Kosley, Jr., G. J. O'Malley, B. Spahl, and K. B. Seamon. (Aminoalkyl)carbamates of forskolin: intermediates for the synthesis of functionalized derivatives of forskolin with different specificities for adenylyl cyclase and the glucose transporter. *J. Med. Chem.* **34**:3204–3212 (1991).
23. Tinari, S. C., and K. A. Suprenant. A pH and temperature-dependent cycling method that doubles the yield of microtubule protein. *Anal. Biochem.* **215**:96–103 (1993).
24. Vallee, R. B. Reversible assembly purification of microtubules without assembly-promoting agents and further purification of tubulin, microtubule-associated proteins, and MAP fragments. *Methods Enzymol.* **134**:89–104 (1986).
25. Olmsted, J. B., D. L. Semple, W. M. Saxton, B. W. Neighbors, and J. R. McIntosh. Cell cycle-dependent changes in the dynamics of MAP2 and MAP4 in cultured cells. *J. Cell Biol.* **109**:211–223 (1989).
26. Mareel, M. M., G. A. Storme, C. H. Dragonetti, G. K. De Bruyne, B. Hartley-Asp, J. L. Segers, and M. L. Rabaey. Antiinvasive activity of estramustine on malignant MO_4 mouse cells and on DU-145 human prostate carcinoma cells *in vitro*. *Cancer Res.* **48**:1842–1849 (1988).
27. Sheridan, V. R., L. A. Speicher, and K. D. Tew. The effects of estramustine on mitotic progression in DU 145 human prostatic carcinoma cells. *Eur. J. Cell Biol.* **54**:268–276 (1991).
28. Robol, A., K. Gull, and C. I. Pogson. Evidence that griseofulvin binds to a microtubule-associated protein. *FEBS Lett.* **75**:149–152 (1977).
29. Sloboda, R. D., G. Van Blaricom, W. A. Creasey, J. L. Rosenbaum, and S. E. Malawista. Griseofulvin: association with tubulin and inhibition of *in vitro* microtubule assembly. *Biochem. Biophys. Res. Commun.* **105**:882–888 (1982).
30. Gupta, R. S. Griseofulvin resistance mutation of Chinese hamster ovary cells that affects the apparent molecular weight of a ≃200,000-dalton protein. *Mol. Cell. Biol.* **4**:1761–1768 (1984).
31. Cabral, F., M. E. Sobel, and M. M. Gottesman. CHO mutants resistant to colchicine, colcemid or griseofulvin have an altered β-tubulin. *Cell* **20**:29–36 (1980).
32. Vandre, D. D., V. E. Centonze, J. Peloquin, R. M. Tombes, and G. G. Borisy. Proteins of the mammalian mitotic spindle: phosphorylation/dephosphorylation of MAP-4 during mitosis. *J. Cell Sci.* **98**:577–588 (1991).

Send reprint requests to: Kenneth D. Tew, Department of Pharmacology, Fox Chase Cancer Center, 7701 Burholme Ave., Philadelphia, PA 19111.